IEEE Access
Multidisciplinary | Rapid Review | Open Access Journal

Received April 26, 2019, accepted May 16, 2019, date of current version June 19, 2019.

Digital Object Identifier 10.1109/ACCESS.2019.2919700

ADMM-Based Distributed Optimization of Hybrid MTDC-AC Grid for Determining Smooth Operation Point

SADDAM AZIZ[1], (Student Member, IEEE), JIANCHUN PENG[2], (Senior Member, IEEE), HUAIZHI WANG[2], (Member, IEEE), AND HUI JIANG[1]

[1]College of Optoelectronic Engineering, Shenzhen University, Shenzhen 518060, China
[2]College of Mechatronics and Control Engineering, Shenzhen University, Shenzhen 518060, China

Corresponding authors: Huaizhi Wang (wanggb@szu.edu.cn) and Hui Jiang (huijiang@szu.edu.cn)

This work was supported in part by the National Natural Science Foundations of China under Grant 51707123, in part by the Natural Science Foundations of Guangdong Province under Grant 2016A030313041, and in part by the Foundation of Shenzhen Science and Technology Committee under Grant JYCJ20180305125407996.

ABSTRACT Accompanied by the rising fashion of distributed energy resources requiring distributed optimization is becoming more prevalent among power system. However, research for distributed optimization to determine smooth operation point (SOP) has attracted less attention in hybrid multi-terminal high voltage direct current (MTDC) and thus, it is still a core issue. The proposed method mainly designed to deal with SOP, and this goal can be mainly achieved by taking minimal line losses and smoothness objectives (MLLSO), which is formulated as an MLLSO optimization model. Then, the MLLSO optimization is transformed to single-objective distributed optimization through weight normalization of both objective functions. A minimal line loss objective and smoothness objective-based optimal power flow (MLLOSOBOPF) model is built at first to effectively handle prevailing constraints for the power systems parameters. Then, the alternating direction method of multipliers (ADMM) is utilized to solve this model by breaking it into smaller pieces based on OPF, each of which is easier to handle. In addition, different sized power systems are integrated with the 14-bus and 30-bus hybrid MTDC-AC systems to increase the complexity of test systems. Finally, based on 14-bus and 30-bus hybrid MTDC-AC systems, the computational output and comparison of the proposed method with centralized optimization centralized MTDC show that the proposed method is feasible and effective for determining hybrid MTDC grid SOP.

INDEX TERMS Distributed optimization, smooth operation, multi terminal DC (MTDC), optimal power flow (OPF).

I. INTRODUCTION

The modern technological evolution and the increasing issues of global warming have inspired researchers to search for cleaner and better productive networks [1]–[3]. One of the best effective ways to reduce the impacts of fossil fuels on the nature is to produce energy from the cleaner energy sources [4], which are located near to the users [5], [6] such as wind turbines, photovoltaic panels, and fuel cells [7]. These sources are known as Distributed Generation (DG) units.

As the climate problems draw great common concern of public, the technology of Distributed Generation (DG) has grown tremendously [8], [9] and further DGs will be connected to the distribution networks [10]–[12]. With increasing penetrations of distributed energy resources (e.g., rooftop PV generation, battery energy storage, plug-in vehicles with vehicle-to-grid capabilities, controllable loads providing demand response resources, etc.), the centralized paradigm most prevalent in current power systems will potentially be augmented with distributed optimization algorithms. Rather than collecting all problem parameters and performing a central calculation, distributed algorithms are computed by many agents that obtain certain problem parameters via communication with a limited set of neighbors. Depending on the specifics of the distributed algorithm and the application of interest, these agents may represent individual buses or large portions of a power system.

The associate editor coordinating the review of this manuscript and approving it for publication was Fabio Massaro.

Distributed algorithms have several potential advantages over centralized approaches. The computing agents only have to share limited amounts of information with a subset of the other agents. This can improve cybersecurity and reduce the expense of the necessary communication infrastructure. Distributed algorithms also have advantages in robustness with respect to failure of individual agents. Further, with the ability to perform parallel computations, distributed algorithms have the potential to be computationally superior to centralized algorithms, both in terms of solution speed and the maximum problem size that can be addressed. Finally, distributed algorithms also have the potential to respect privacy of data, measurements, cost functions, and constraints, which becomes increasingly important in a distributed generation scenario. Although AC technology is dominant in today's electric power system but DC technology and its rapid growth over the past two decades in power systems applications at different voltage levels is obvious as well. As a result, there is a paradigm shift from bulk central power systems to a huge number of smaller distributed renewable power systems [13], [14] and the replacement of centralized optimization by a more distributed optimization. These reasons are precursor to establish the proposed idea. AC and DC transmission systems coexisted since the initiation period of the electrical grid [15]. The efficiency of the hybrid system in case of AC and DC systems is discussed in [16]. The utilization of hybrid MTDC-AC to boost the transient stability of the AC system is shown in [17], [18]. The concept of hybrid MTDC-AC for multi-infeed to AC networks is discussed in [19], [20]. Hybrid HVDC systems with AC and DC [17], [20]–[26] can unite the pros of both systems.

While the attention toward hybrid-MTDC networks is accelerating, there are still numerous features of these networks that require additional research. The key feature is related to their power loss reduction and smoothness. The core issue is regulation of the dc-voltage in hybrid MTDC-AC networks in terms of smoothness, as it has direct connection with the power flow and power balance, and frequency in ac grids. However, dissimilar frequency that is a worldwide parameter, the dc grid's voltage differs throughout the network depending on power which is injected at each node. Currently, there are no exact paradigms that govern the smoothing process in hybrid MTDC-AC grid. So, various techniques are applied relying on combination of centralized control and decentralized control, or separately both can be explored in [27]–[29]. A hierarchical OPF scheme is recommended in [30] to handle the unbalanced setup, where the networks are divided into several areas and regional coordinators are needed. A complete distributed algorithm is designed in [30], where the smoothness for distributed optimization is not considered. To tackle this problem, proposed distributed optimization approach that has ability to divide the optimal power flow into sub problems.

Therefore, this research is devoted to scrutinizing ADMM based distributed optimization and MLLSO optimization techniques for hybrid MTDC grids. Compared with existing researches on similar fields, the contributions of this paper can be summarized as below. Firstly, a new objective function is proposed to make the power system smooth at different scenarios. Secondly, distributed method based on ADMM algorithm is applied to solve optimization problems by splitting them into smaller pieces, which make easier to determine hybrid MTDC smooth operation point. Finally, the validation and the effectiveness of proposed model and methods on modified IEEE14 and IEEE 30 bus systems integrated with wind turbine. The achieved results make sure that proposed method has the potential to handle the distribution optimization and MLLSO optimization problems in hybrid MTDC-AC grid. As a result, it is worthwhile to study the problem of voltage smoothing.

In this paper, proposed method promises distributed optimization for determining hybrid MTDC smoothness operation point under a variety of operation scenarios and time-scales. Therefore, there is no need to utilize the communication channels as hybrid-MTDC systems can remain in operational mode without them. So, it will be also helpful while we are extending hybrid MTDC-AC system. The remaining paper is consisting of these sections. The mathematical modeling in section II and ADMM based distributed approach in section III, case study and simulation and results are discussed in section IV. Conclusion of the proposed method is made in Section IV.

II. MULTI-OBJECTIVE MODELING OF THE HYBRID MTDC/AC GRID

The first objective is to minimize the smoothness of the hybrid MTDC-AC system, as the state transition is based on voltage vector, that's why considered it for the sake of making the transition of the hybrid MTDC-AC grid states smoother throughout one-hour dispatch time interval, we build the following objective function (1) where V_t and V_{t-1} are the voltage at current time and voltage at previous time interval respectively.

$$\min f_1(x) = |V_t - V_{t-1}| \tag{1}$$

The second objective is to reduce the power loss in hybrid MTDC-AC system. There are two bus systems shown in Fig. 2 and Fig. 3. In the Fig. 2 14 bus hybrid MTDC-AC test system is consist of two subsystems and in the Fig. 3 the 30-bus hybrid MTDC-AC test system is with three subsystems. However, both bus test systems are same in terms of AC and DC buses combination, therefore the same objective function is defined separately for AC and DC case shown in below equations (2) and (9).

A. FOR AC CASE

Mainly the system is consisting of AC and DC subsystems, so firstly, AC system is taken under consideration.

a) Objective function

$$\min f_2(x) = P_{Loss} = \sum_{(i,j)\in K} g_{ij}(V_i^2 + V_j^2 - 2V_iV_jcos\theta_{ij}) \tag{2}$$

where $K \in \{1, 2, 3, \ldots\ldots, m\}$ and i, j$\{1, 2, \ldots, n\}$

b) Equality Constraints

$$V_i \sum_{j=1}^{N} V_j \left(G_{ij} cos\theta_{ij} + B_{ij} sin\theta_{ij}\right) + P_{LI} - P_{Gi} = 0 \quad (3)$$

$$V_i \sum_{j=1}^{N} V_j \left(G_{ij} sin\theta_{ij} - B_{ij} cos\theta_{ij}\right) + Q_{LI} - Q_i = 0 \quad (4)$$

Now P_{Gi} and Q_{Gi} are the active and reactive power generations of bus i; P_{Li} and Q_{Li} are the active and reactive power loads of bus i; θ_{ij} is the voltage angle difference between bus i and j, and G_{ij} and B_{ij} are transfer admittance from bus i to bus j.

c) Inequality constraints

Generation limits, voltage limits and current limits are chosen here as inequality constraints respectively in equation (5) to equation (8) accordingly.

$$P_{Gi}^{\min} \le P_{Gi} \le P_{Gi}^{\max}, \quad i = 1, 2, 3, \ldots\ldots, n_G \quad (5)$$

$$Q_{Gi}^{\min} \le Q_{Gi} \le Q_{Gi}^{\max}, \quad i = 1, 2, 3, \ldots\ldots, n_G \quad (6)$$

$$V_i^{\min} \le V_i \le V_i^{\max}, \quad i = 1, 2, 3, \ldots\ldots, n_G \quad (7)$$

$$-I_{ij}^{\min} \le I_{ij} \le I_{ij}^{\max}, \quad i = 1, 2, 3, \ldots\ldots, n_G \quad (8)$$

B. FOR DC CASE

The operation state of the power system can be defined by the set of P-V droop control reference voltage values of the hybrid MTDC- AC grid. As expressed in circuit theory, bus voltage vector determines the base operational point. Where the power system transfers first base operational point to final base operational point, the execution of the transition is indicated by the closeness between the base operational points indicates the execution of the transition. The closer distance will cause smaller the step to be transited by all P-V droop controllers, that's why the best of smoothness of the grid state transition between the base operational points. As a result, we take this distributed approach for determining the MTDC grid smooth operation point. Smoothness in distributed manner is one of the key technologies to guarantee reliable and economic smooth operation [31].

a) *Objective function*

$$\min f_2(x) = \sum_{j=1}^{n} g_{ij} * (V_i - V_j)^2 \quad (9)$$

where, $i, j = 1, 2, \ldots, n$.

The circuit laws govern the state of the MTDC grid. So, the adjustment of the set of P-V droop control reference voltage values or the base operation point should fulfil requirements of all bus MW balance equations. Further, limit the device rated voltage and DC line permissible maximum current, voltage and current related security constraints should be considered while deciding the base operation point.

b) *Equality constraints*

$$s.t. \sum_{j=1}^{n} V_{ki}(V_{ki} - V_{kj}) g_{ij} - P_{Gki} + P_{Dki} = 0 \quad (10)$$

Power injection at the load buses is taken as equality constraints. So, equality constraints are in the form of Bus Megawatt (MW) balance equation. In the equation (10), the equality constraints of the optimization problem consist of power injected at each node of the system and the load level of the system. The equation (9) shows that the power flow at each node, where g_{ij} is the conductance of the all branches of the network. Likewise, $V_i - V_j$ is difference of voltage magnitude at node i to node.

c) *Inequality constraints.*

$$P_{Gi}^{\min} \le P_{Gi} \le P_{Gi}^{\max} \quad (11a)$$

$$-I_{ij\max} \le g_{ij} * (V_i - V_j) \le I_{ijmax} \quad (11b)$$

$$V_i^{\min} \le V_i \le V_i^{\max} \quad (12)$$

where $k \in \{1, 2, 3, \ldots, m\}$ and $i, j \in \{1, 2 \ldots, n$ and P_{Loss} is the power loss in (i, j) nodes, K and $(i, j) \in K$, indicates the set of branches of the MTDC system and both are the (i, j) nodes of a branch. V_i and V_j represents voltage magnitude of node (i, j). The conductance between nodes (i, j) is g_{ij}.

III. ADMM BASED DISTRIBUTED OPTIMIZATION

Normalization of MLLSO objectives is expressed in equation form as:

$$F_{(x)} = \lambda_1 \min f_1(x) + \lambda_2 \min f_2(x) \quad (13)$$

Notation $F(x)$ represents the sum of both objectives smoothness and power loss. λ_1 and λ_2 show the weightage of given objective functions $\min f_1(x)$ and $\min f_2(x)$. It is obvious $F(x)$ achieves the minimum value, the transition between different states of the grid will be smoothest. So, we should minimize $F(x)$ in determining base operation point.

The converter is supposed to be lossless, that's why the power on both directions of the converter is constraint as follows:

$$P_{AC_{conveter}} = P_{DC_{conveter}} \quad (14)$$

where, active power into the converter is $P_{AC_{conveter}}$ and the output of the converter in terms of DC power flowing is $P_{DC_{conveter}}$. The Kirchhoff's voltage law condition must be fulfilled by the DC voltage magnitude.

$$V_{DC_j} - V_{R_{DC}} - V_{DC_k} = 0 \quad (15)$$

The DC voltage magnitude of the rectifier in the above equation written as V_{DC_i}, $V_{R_{DC}}$ and V_{DC_k} are the voltage drop caused by the DC line and the invert's DC voltage magnitude respectively.

How much active power is to be transmitted over the DC line is controlled by rectifier, considering that the DC voltage at its node is controlled by inverter. Both converters can handle either the AC voltage, or the injected reactive power Q, respectively. The possible rate of power transition over the DC line, as seen in figure 1 can be written

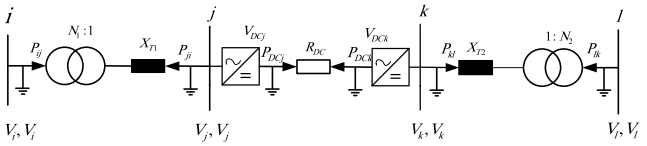

FIGURE 1. DC line's model.

as follows [33].

$$P_{il} = P_{ij} = N_1^{-2} V_i^2 g_{T1} - N_1^{-1} V_i V_j (g_{T1} \mathrm{Cos}(\theta_i - \theta_j) + b_{T1} \mathrm{Sin}(\theta_i - \theta_j)) \quad (16)$$

$$Q_{il} = P_{ij} = -N_1^{-2} V_i^2 b_{T_1} + N_1^{-1} V_i V_j (b_{T_1} \mathrm{Cos}(\theta_i - \theta_j) - g_{T_1} \mathrm{Sin}(\theta_i - \theta_j)) \quad (17)$$

where $Y_{T_1} = (Z_{T_1})^{-1} = g_{T_1} + j y_{T_1}$ is admittance of the coupling transformer. The power flow into the converter is as follow:

$$P_{ji} = V_j^2 g_{T1} - N_1^{-1} V_i V_j (g_{T1} \mathrm{Cos}(\theta_j - \theta_i) + b_{T1} \mathrm{Sin}(\theta_j - \theta_i)) \quad (18)$$

$$Q_{ji} = -V_j^2 b_{T1} + N_1^{-1} V_i V_j (b_{T_1} \mathrm{Cos}(\theta_j - \theta_i) - g_{T_1} \mathrm{Sin}(\theta_j - \theta_i)) \quad (19)$$

Because it is supposed that the converter is to be lossless, the power on each side of the converter is given by:

$$P_{DCx} = -P_{ji} \quad (20)$$

$$P_{DCy} = -P_{kl} \quad (21)$$

Both production or dissipation of reactive are caused by converter power, the reactive power on converter can only be constrained as:

$$Q_{ji_{\min}} \leq Q_{ji} \leq Q_{ji_{\max}} \quad (22)$$

$$Q_{kl_{\min}} \leq Q_{kl} \leq Q_{kl_{\max}} \quad (23)$$

As a result, following power balance at rectifier bus i:

$$P_i + P_{gen,i} - P_{ij} - P_{Load,i} = 0 \quad (24)$$

$$Q_i + Q_{gen,i} - Q_{ij} - Q_{Load,i} = 0 \quad (25)$$

and for the inverter bus l:

$$P_l + P_{gen,l} - P_{lk} - P_{Load,l} = 0 \quad (26)$$

$$Q_l + Q_{gen,l} - Q_{lk} - Q_{Load,l} = 0 \quad (27)$$

For the internal rectifier bus x, the following power equation are derived:

$$P_{ji} + P_{DCj} = 0 \quad (28)$$

P_{DCj} can be calculated directly by P_{ij}. The power over the DC link is controlled by $P_{il} = P_{ij}$ and therefore P_{ij} is the negative value of the controlled power flow minus the losses of the coupling transformer. For the internal inverter bus j, the following power equation is derived:

$$P_{kl} = -P_{DCk} \quad (29)$$

The DC power P_{DCk} which flows into the inverter side can be calculated as follows:

$$P_{DCk} = -(P_{DCj} - P_{R_{DC}}) \quad (30)$$

$$P_{DCk} = -(P_{DCj} - \frac{V_{R_{DC}}^2}{R_{DC}}) \quad (31)$$

With equation (15) the voltage losses over the DC resistance, $V_{R_{DC}}$ can be expressed with V_{DCj} and V_{DCk}.

$$P_{DCk} = -(P_{DCj} - \frac{(V_{DCj} - V_{DCk})^2}{R_{DC}}) \quad (32)$$

This leads to following power equation at bus k:

$$P_{km} - (P_{DCj} - \frac{(V_{DCj} - V_{DCk})^2}{R_{DC}}) = 0 \quad (33)$$

With Kirchhoff's Law from equation (15) the following DC voltage equation can be derived:

$$V_{DCj} - V_{R_{DC}} - V_{DCk} = 0 \quad (34)$$

$$V_{DCj} - R_{DC} I_{DC} - V_{DCk} = 0 \quad (35)$$

I_{DC} can be calculated as

$$I_{DC} = \frac{P_{DC_j}}{V_{DCj}} - V_{DCk} = 0 \quad (36)$$

And therefore

$$V_{DC_j} = \frac{P_{DC_j} R_{DC}}{V_{DCj}} - V_{DCk} = 0 \quad (37)$$

The primary aim of the proposed approach is to break the OPF into separate subproblems through ADMM algorithm, each of which contains only a smaller subset of the variables to be optimized with limited overlap among each other. For example, nodes of the power system in topographical proximity are set together, and limited common variables are only shared by adjacent partitions. The theme is then to solve the constrained sub-problems with respect to the subset of variables using, during applying the consistency of the overlapping variables by making them identical to some dummy variables through the equality constraints. These steps can be repeated, which leads to distributed implementation. More precisely, the objective function and constraints of the OPF can be break into N sub-systems:

$$\min F(x) = \sum_{n=1}^{N} F_n(x_n) \quad (38)$$

$$s.t.\ C_{eq}(x) = [c_{eq,1}(x_1)^T, c_{eq,2}(x_2)^T, \ldots, c_{eq,}(x_N)^T]^T = 0 \quad (39)$$

$$C_{i_eq}(x) = [c_{i_eq,1}(x_1)^T, \ldots, c_{i_eq,N}(x_N)^T]^T \leq 0 \quad (40)$$

$$x_{n,lb} \leq x_n \leq x_{n,ub}, \quad n = 1, 2, 3, \ldots, N. \quad (41)$$

where x_n is a small subset of variables in x with lower and upper-bound as $x_{n,lb}$ and $x_{n,ub}$ respectively However, $F_n(x_n), C_{eq,n}(x_n), C_{i_eq,n}(x_n)$ depend only x_n. Commonly, the decomposition is performed in a way such that x_n only

contains a small subset of variables in x with limited overlapping with each other. Precisely, S_n denote the selection matrix which extracts the subset x_n from x with variables appearing in the same precedence order. Thus,

$$\tilde{x}_n = \tilde{z}_n x, \quad n = 1, 2, \ldots, N. \tag{42}$$

The selection matrix extracting the overlapping variables $\tilde{x}_n$ from x_n with variables appearing in the same precedence order as in x is denoted as F_n. Therefore,

$$\tilde{x}_n = F_n x_n \tag{43}$$

The problem in (38)-(41) can be decoupled by defining a dummy variable Z with nonzero entries only at the locations corresponding to the overlapping variables in Z and the introduction of consensus constraints on the dummy variables between the partitions. Here, we remark that Z is used to simplify the mathematical formulation. In practice, each subsystem can still access their own overlapping variables without forming the whole vector Z. Instead, they can use

$$\tilde{z}_n = F_n S_n z = \tilde{S}_n z \tag{44}$$

Using (43) and (44), the OPF in (38)-(41) can be re-written as

$$\min_x F(x) = \sum_{n=1}^{N} F_n(x_n), \tag{45}$$

$$s.t.\ C_{eq,n}(x_n) = 0,\ C_{i_eq,n}(x_n) = 0, \quad x_{n,lb} \le x_n \le x_{n,ub}, \tag{46}$$

$$\tilde{x}_n = \tilde{z}_n x, \quad n = 1, 2, \ldots, N. \tag{47}$$

One can see that each partition can solve a smaller constrained optimization in the variable x_n subject to the consensus constraints in (47). Similar decomposition is also used in [33], [34]. The augmented Lagrangian method can be used to absorb the linear consensus constraints into the objective function subject to the nonlinear constraints in (46) which yields

$$\min_{x,\tilde{Z},\lambda} \sum\nolimits_{n=1}^{N} L_{A,n}(x_n, \tilde{z}_n, \lambda_n, \rho) \tag{48}$$

$$C_{eq,n}(x_n) = 0,\ C_{i_eq,n}(x_n) = 0, \quad x_{n,lb} \le x_n \le x_{n,ub}, \tag{49}$$

where

$$L_{A,n}(x_n, \tilde{z}_n, \lambda_n, \rho) = F_n(x_n) + \lambda_n^T(\tilde{x}_n - \tilde{z}_n) + \frac{1}{2}\rho \times \| \tilde{x}_n - \tilde{z}_n \|^2, \lambda = [\lambda_1^T, \ldots \lambda_T^T]^T \tag{50}$$

λ_n is the Lagrange multiplier in the nth partition and ρ is an augmented Lagrangian penalty parameter. Then, (48) and (49) can be solved using the following iterative procedure where each subproblem can be solved in a distributed manner.

$$x_n^{(t+1)} = \operatorname*{argmin}_{x_n} L_{A,n}(x_n, \tilde{z}_n^{(t)}, \lambda_n^{(t)}, \rho) \tag{51a}$$

$$s.t.\ C_{eq,n}(x_n) = 0,\ C_{i_eq,n}(x_n) = 0,\ x_{n,lb} \le x_n \le x_{n,ub}, \tag{51b}$$

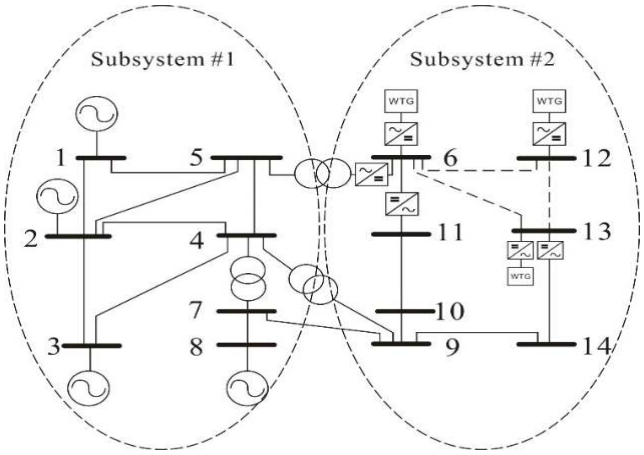

FIGURE 2. 14 Bus hybyrid mtdc-ac system.

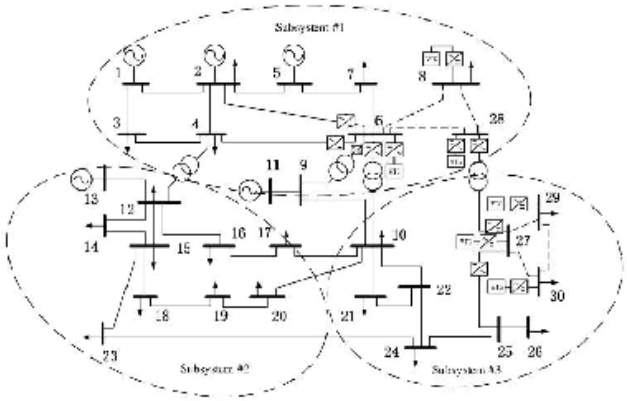

FIGURE 3. 30 Bus hybyrid mtdc-ac system.

$$\tilde{z}_n^{(t+1)} = \operatorname*{argmin}_{x_n} \sum_{n=1}^{N} (\lambda_n^T(x_n^{(t+1)} - \tilde{z}_n) + \frac{1}{2}\rho(x_n^{(t+1)} - \tilde{z}_n) \|^2), \tag{52}$$

$$\lambda_n^{(t+1)} = \lambda_n^{(t)} + \rho(\tilde{x}_n^{(t+1)} - \tilde{z}_n^{(t+1)}), \quad n = 1, 2, \ldots, N. \tag{53}$$

From (51) to (51c), we can see that (51c) contains N independent least squares (LS) problems and its analytical solution is given as

$$\tilde{z}_k^{(t+1)} = D^{-1} \sum_{n \in N} \tilde{E}_n \tilde{x}_n^{(t+1)}, \quad n = 1, \ldots, N. \tag{54}$$

where $\tilde{x}_n$ is an expansion matrix mapping the overlapping variables in the *n-th* partition back to the variable x while keeping other variables at *zero*. The (j, j) entry of the diagonal matrix D equals to the number of times that $j - th$ variable appears as an overlapping variable in all N subsystems. In this way, the overlapping variables from K are averaged to obtain the global variables. The K independent constrained sub-problems in (51) can be solved using the distributed approach, which solves the sub-problem

TABLE 1. 14 Bus voltage level method 1.

Centralized OPF Method					
Bus #	Scen.1	Scen.2	Scen.3	Scen.4	Scen.5
1	1.0598	1.0549	1.0519	1.0497	1.0479
2	1.0555	1.0504	1.0474	1.0451	1.0432
3	1.0549	1.0499	1.0469	1.0447	1.0428
4	1.0497	1.0459	1.0437	1.042	1.0406
5	1.0513	1.0472	1.0447	1.0429	1.0414
6	1.0339	1.0304	1.0278	1.0258	1.0245
7	1.0309	1.03	1.0295	1.0291	1.0288
8	1.0600	1.06	1.0599	1.0599	1.0599
9	1.0129	1.0121	1.0117	1.0114	1.0112
10	1.0075	1.0066	1.0062	1.0059	1.0056
11	1.013	1.0109	1.0098	1.009	1.0083
12	1.0370	1.0373	1.0331	1.0293	1.0294
13	1.0308	1.0299	1.0265	1.0236	1.0233
14	0.9965	0.997	0.9962	0.9955	0.9957

TABLE 2. 30 Bus voltage level method 1.

Centralized OPF Method					
Bus #	Scen.2	Scen.2	Scen.3	Scen.4	Scen.5
1	1.0510	1.0523	1.0532	1.0540	1.0543
2	1.0467	1.0479	1.0487	1.0494	1.0498
3	1.0464	1.0479	1.049	1.0499	1.0503
4	1.0441	1.0456	1.0467	1.0476	1.048
5	1.0456	1.0475	1.0484	1.0491	1.0495
6	1.0599	1.0598	1.0596	1.0594	1.0596
7	1.0382	1.0403	1.0416	1.0426	1.0431
8	1.0599	1.0597	1.0594	1.0592	1.0595
9	1.0267	1.0292	1.0309	1.0323	1.0328
10	1.0069	1.0103	1.0126	1.0145	1.0154
11	1.0600	1.0600	1.0600	1.0600	1.0600
12	1.0158	1.018	1.0197	1.0210	1.0215
13	1.0305	1.031	1.0316	1.0322	1.0320
14	1.0006	1.0037	1.006	1.0078	1.0086
15	0.9969	1.0003	1.0027	1.0048	1.0056
16	1.0047	1.0077	1.01	1.0118	1.0126
17	1.0009	1.0044	1.0069	1.0089	1.0099
18	0.9878	0.9918	0.9947	0.9971	0.9982
19	0.9857	0.9899	0.993	0.9954	0.9966
20	0.9902	0.9942	0.9972	0.9995	1.0006
21	0.9942	0.9981	1.001	1.0033	1.0043
22	0.9948	0.9987	1.0015	1.0038	1.0048
23	0.9873	0.9913	0.9942	0.9966	0.9976
24	0.9832	0.9876	0.9908	0.9934	0.9945
25	0.9976	1.0011	1.0038	1.0061	1.0067
26	0.9795	0.984	0.9874	0.9902	0.9912
27	1.0107	1.0135	1.0157	1.0177	1.0177
28	1.0598	1.0599	1.06	1.0599	1.0599
29	1.0131	1.0175	1.0211	1.0241	1.0227
30	1.0063	1.0113	1.0154	1.0187	1.0172

in (51) by applying Newton's method to the Karush–Kuhn–Tucker (KKT) conditions of (51). More specifically, at the $r-th$ inner iteration of (51) denoted by $x_n^{(t)(r)}$, we aim to solve the following quadratic programming sub-problem to find the search direction. For $r = 0, 1, \ldots$.

$$d_n^{(t)(r+1)} = \operatorname{argmin} \frac{1}{2} d_n^t H^{(t)(r)} d_n + \nabla L_{A,n}(x_n^{(t)(r)}) d_n, \quad (55)$$

$$s.t.\ \nabla c_{eq,n}(x_n)^T d_n + c_{eq,n}(x_n) = 0, \quad (56)$$

$$\nabla c_{i\_eq,n}(x_n)^T d_n + c_{i\_eq,n}(x_n) \leq 0, x_n \in [x_{k,lb}, x_{k,ub}] \quad (57)$$

TABLE 3. 14 Bus voltage level method 2.

Centralized MTDC Method					
Bus #	Scen.1	Scen.2	Scen.3	Scen.4	Scen.5
1	1.0598	1.0598	1.0598	1.0598	1.0598
2	1.0555	1.0555	1.0554	1.0554	1.0554
3	1.0549	1.0549	1.0549	1.0549	1.0549
4	1.0497	1.0497	1.0497	1.0500	1.0500
5	1.0513	1.0514	1.0518	1.0518	1.0519
6	1.0339	1.0304	1.0311	1.0317	1.0304
7	1.0309	1.0309	1.0309	1.0309	1.0309
8	1.0600	1.0569	1.0541	1.0531	1.0521
9	1.0129	1.0129	1.013	1.0137	1.0137
10	1.0075	1.0078	1.0079	1.0089	1.0089
11	1.0130	1.013	1.013	1.0137	1.0137
12	1.0370	1.037	1.0361	1.0347	1.0347
13	1.0308	1.0292	1.0292	1.0282	1.0277
14	0.9965	0.9975	0.9982	0.9992	0.9995

TABLE 4. 30 bus voltage level method 2.

Centralized MTDC Method					
Bus #	Scen.2	Scen.2	Scen.3	Scen.4	Scen.5
1	1.0510	1.0523	1.0532	1.0540	1.0543
2	1.0467	1.0479	1.0487	1.0494	1.0498
3	1.0464	1.0479	1.049	1.0499	1.0503
4	1.0441	1.0456	1.0467	1.0476	1.048
5	1.0456	1.0475	1.0484	1.0491	1.0495
6	1.0599	1.0598	1.0596	1.0594	1.0596
7	1.0382	1.0403	1.0416	1.0426	1.0431
8	1.0599	1.0597	1.0594	1.0592	1.0595
9	1.0267	1.0292	1.0309	1.0323	1.0328
10	1.0069	1.0103	1.0126	1.0145	1.0154
11	1.0600	1.0600	1.0600	1.0600	1.0600
12	1.0158	1.018	1.0197	1.0210	1.0215
13	1.0305	1.031	1.0316	1.0322	1.0320
14	1.0006	1.0037	1.006	1.0078	1.0086
15	0.9969	1.0003	1.0027	1.0048	1.0056
16	1.0047	1.0077	1.01	1.0118	1.0126
17	1.0009	1.0044	1.0069	1.0089	1.0099
18	0.9878	0.9918	0.9947	0.9971	0.9982
19	0.9857	0.9899	0.993	0.9954	0.9966
20	0.9902	0.9942	0.9972	0.9995	1.0006
21	0.9942	0.9981	1.001	1.0033	1.0043
22	0.9948	0.9987	1.0015	1.0038	1.0048
23	0.9873	0.9913	0.9942	0.9966	0.9976
24	0.9832	0.9876	0.9908	0.9934	0.9945
25	0.9976	1.0011	1.0038	1.0061	1.0067
26	0.9795	0.984	0.9874	0.9902	0.9912
27	1.0107	1.0135	1.0157	1.0177	1.0177
28	1.0598	1.0599	1.06	1.0599	1.0599
29	1.0131	1.0175	1.0211	1.0241	1.0227
30	1.0063	1.0113	1.0154	1.0187	1.0172

After obtaining the search direction $d_n^{(t)(r+1)}$, the iterate $x_n^{(t)(r)}$ could be updated by a line search method, i.e. $x_n^{(t)(r+1)} = x_n^{(t)(r)} + \alpha^{(t)(r)} d_n^{(t)(r+1)}$, where $\alpha^{(t)(r)}$ is a step-size obtained from line-search [35]. Suppose the distributed convergence at iteration R, we update the $x_n^{(t+1)}$ in equations (51) to (51c) is to achieve a sufficiently small l_2 norm of the following vector

$$\varepsilon_n^t = [(\tilde{z}_n^{(t+1)} - \tilde{z}_n^{(t)})^T, (\tilde{z}_n^{(t+1)} - \tilde{x}_n^{(t)})^T]^T \quad (58)$$

TABLE 5. 14 Bus voltage level method 3.

Distributed MTDC Method					
Bus #	Scen.1	Scen.2	Scen.3	Scen.4	Scen.5
1	1.0558	1.0558	1.0558	1.0558	1.0558
2	1.0506	1.0506	1.0506	1.0501	1.0501
3	1.0501	1.0501	1.0501	1.0501	1.0501
4	1.0443	1.0446	1.0449	1.0452	1.0452
5	1.0457	1.0457	1.0457	1.0457	1.0457
6	1.0280	1.0243	1.025	1.0259	1.0245
7	1.0291	1.0307	1.0307	1.0307	1.0311
8	1.0600	1.0600	1.0600	1.0568	1.0568
9	1.0088	1.0085	1.0085	1.0085	1.0085
10	1.0031	1.0031	1.0033	1.0036	1.0037
11	1.0077	1.0077	1.0077	1.008	1.0081
12	1.0312	1.0312	1.0303	1.0294	1.0294
13	1.0250	1.0237	1.0237	1.0237	1.0232
14	0.9917	0.9924	0.9931	0.9937	0.9940

TABLE 6. 30 Bus voltage level method 3.

Distributed MTDC Method					
Bus #	Scen.1	Scen.2	Scen.3	Scen.4	Scen.5
1	1.0549	1.0549	1.0551	1.0551	1.0551
2	1.0503	1.0503	1.0503	1.0503	1.0503
3	1.0517	1.0517	1.0517	1.0517	1.0517
4	1.0497	1.0496	1.0495	1.0495	1.0495
5	1.0494	1.0494	1.0494	1.0494	1.0494
6	1.0598	1.0598	1.0598	1.0598	1.0598
7	1.0425	1.0426	1.0427	1.0428	1.0428
8	1.0599	1.0590	1.0583	1.0581	1.0581
9	1.0355	1.0355	1.0355	1.0355	1.0355
10	1.0174	1.0171	1.017	1.0166	1.0166
11	1.0600	1.0586	1.0583	1.0571	1.0571
12	1.0284	1.0276	1.0272	1.0270	1.0270
13	1.0416	1.0416	1.0393	1.0393	1.0393
14	1.0135	1.0135	1.0137	1.0137	1.0137
15	1.0089	1.0092	1.0092	1.0093	1.0093
16	1.0238	1.0243	1.0243	1.0243	1.0243
17	1.0254	1.0254	1.0254	1.0254	1.0254
18	0.9992	0.9996	0.9998	1.0000	1.0000
19	0.9967	0.997	0.9972	0.9974	0.9974
20	1.0009	1.0009	1.0009	1.0009	1.0009
21	1.0051	1.0052	1.0056	1.0056	1.0056
22	1.0058	1.0058	1.0062	1.0062	1.0062
23	0.9990	1.0004	1.0007	1.0007	1.0007
24	0.9955	0.996	0.9967	0.9975	0.9975
25	1.0107	1.0107	1.0107	1.0107	1.0107
26	0.9929	0.9938	0.9944	0.9949	0.9949
27	1.0287	1.0270	1.0257	1.0246	1.0246
28	1.0598	1.0599	1.0599	1.0600	1.0600
29	1.0311	1.0310	1.0310	1.0310	1.0310
30	1.0244	1.0249	1.0253	1.0256	1.0256

IV. CASE STUDIES

The performance of the proposed MLLOSOBOPF approach for distributed optimization has been comprehensively evaluated through 14 and 30 bus hybrid MTDC-AC test system, which are developed and validated by modifying IEEE 14 and 30 bus test systems. To increase systems complexity, the wind turbines are also added with systems. However, to make simulations more realistic, the electric load data from Dongguan City, Guangdong province, China, and the wind power data from the Cathedral Rocks wind farm in Australia are applied. The topology of IEEE 14 and 30 bus test systems can be found in [36]. These hybrid MTDC-AC systems contains two and three systems for 14 and 30 bus systems respectively,

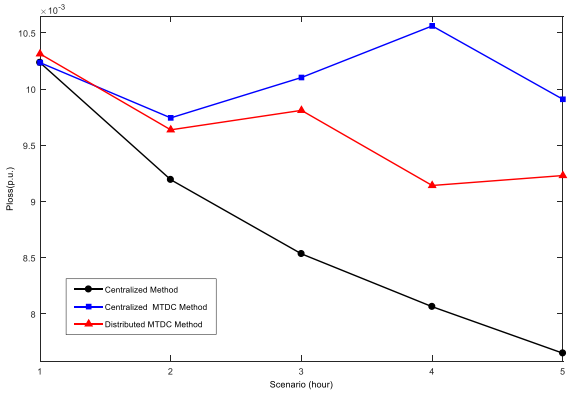

FIGURE 4. Power loss vs scenario, based on 30 bus hybrid MTDC-AC grid.

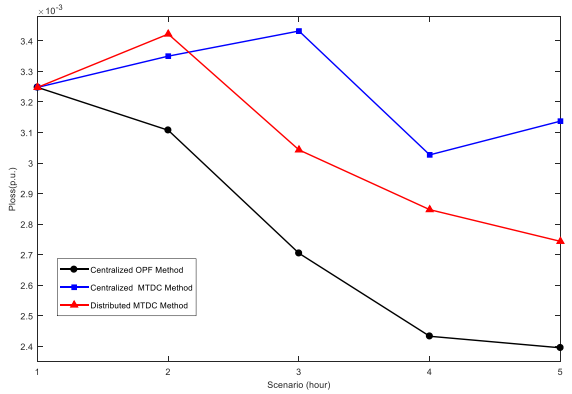

FIGURE 5. Power loss vs scenario, based on 14 bus MTDC-AC grid.

interconnected by converters and transmission lines systems. The same power settings are used for load buses for 14 and 30 bus hybrid MTDC-AC systems as both systems are obtained from 14 and 30 IEEE-bus AC test cases. In the established hybrid MTDC-AC systems, there are 3 and 6 DC line for 14 and 30 bus systems respectively and presented in Fig.2 and Fig.3.

M-file has been implemented in MATLAB®R2016b software to solve the MLLOSOBOPF while considering the centralized OPF method and centralized MTDC method, and distributed MTDC method. All methods are tested on the 14 bus and 30 bus hybrid MTDC-AC test system. Simulations are done using a PC based on AMD A10-7850K Radeon R7, 12 Compute Cores 4C+8G, 3.7 GHz, 8 GB RAM with Windows 10 64-bit operating system. The MLLOSOBOPF is consist of quadratic objective functions and nonlinear constraints.

In this paper, we have taken five operational scenarios, i.e., every adjacent operation scenario interval an hour, all scenarios values vary due the ratios of the wind generations, total load and number of buses. Each output of network's subsections is dependent on the ADMM algorithm and the setpoint of regulating command from the controller according to their respective optimized participating factors. The typical

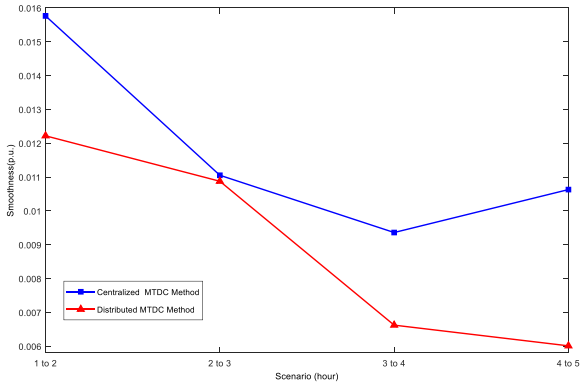

FIGURE 6. Smoothness (P.U) vs scenario based 30 bus MTDC-AC Grid.

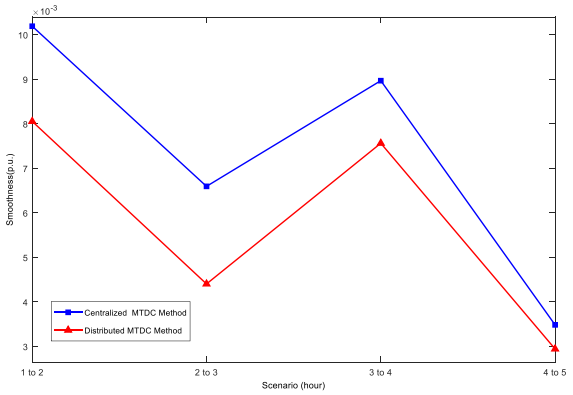

FIGURE 7. Smoothness (P.U) vs scenario based on 14 bus MTDC-AC Grid.

outcomes of 14 and 30 bus hybrid MTDC-AC networks based on MLLSOBOF are shown in Table 5 and 6.

The simulation study case considers the operation of these DC-buses designed for a grid-connected wind generation plant also integrates subsystems. As can be seen in Fig. 2 and Fig. 3. VSCs are connected to the common dc-bus. In which the output of the converter, responsible of managing the DC values through the DC bus. These buses connected power was set equal to the sum of the active and reactive power and the ratings of the generators were affected accordingly. We then solved the MLLOSOBOPF problem by considering each subsection of the network to be governed by an ADMM Algorithm.

The detailed voltage level at five different scenarios against each bus of the whole 14 and 30 bus systems are tabulated in Table 1-6. Table 1, Table 3 and Table 5 indicates 14 bus system, on the other hand Table 2, Table 4 and Table 6 are representing 30 bus system, meanwhile Table 1 - 2, Table 3-4 and Table 5-6 are representing centralized OPF, centralized MTDC and distributed MTDC respectively. Where centralized OPF method, centralized MTDC method and distributed MTDC method are taken as method 1, method 2 and method 3 accordingly.

The comparison of outcomes provided in tables firmly imply that the proposed method yields the same solutions as the centralized method. This validates the accuracy of our method.

The same scenarios were then solved by using a centralized OPF method and centralized MTDC method and the results compared side by side. Both in the centralized method and distributed method, the original nonconvex problem was solved by using an ADMM algorithm, according to section two and three, distributed method-based optimization results are more satisfactory than those obtained by centralized OPF method and centralized MTDC method in terms of voltage regulation.

Fig.4 and Fig.5 show the outcomes of the centralized OPF method, centralized MTDC method and Distributed MTDC method respectively under five scenarios. Both figures are plotted based on scenario (x axis) vs power losses (y axis). Meanwhile, Fig.6 and Fig.7 are showing the outcomes based on method 2 and method 3. Both methods outcomes are plotted in Fig.4-Fig7, we found the outcome values of distributed MTDC method are slightly different than centralized MTDC method and it is some extend neglectable. This makes the proposed method very robust in future smart grid with high diffusion of renewable energies. The prominent performance of the proposed method attributes to its performance capability and adaptiveness over a wide range of power systems.

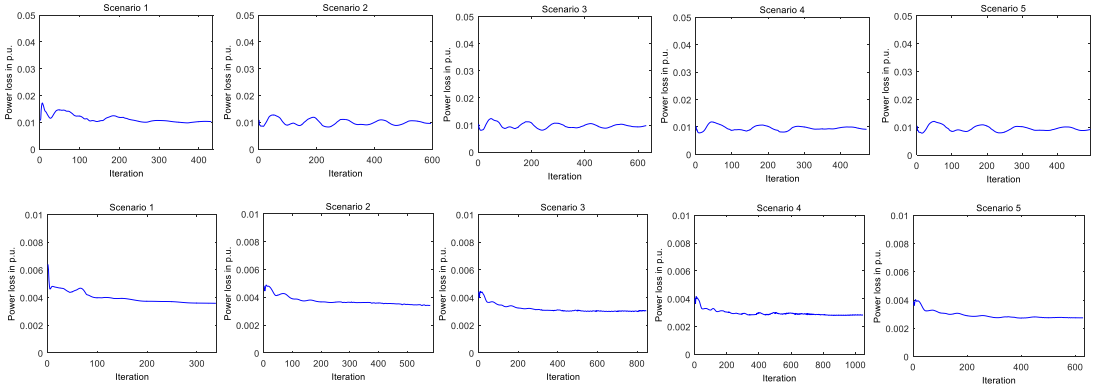

FIGURE 8. Power loss vs iteration based on 30 and 14 bus hybrid MTDC-AC system.

V. CONCLUSION

A Multi-Terminal high voltage direct current hybrid (MTDC)-AC system that encompasses the almost complete range of processes and techniques related to the effective transmission of electricity is an essential feature of future power grid. In this paper, a new approach has been proposed to solve the smoothness problem of a hybrid MTDC-AC system with AC/DC lines. A minimal line loss objective and smoothness objective based optimal power flow is applied first to the distributed optimization approach, such that the problem related to each subsystem can be solved separately. Then, an alternating direction method of multipliers algorithm has been used to efficiently solve the distribution optimization problem for every subsystem in the hybrid MTDC-AC system. The proposed approach has been demonstrated by solving the centralized OPF method, centralized MTDC method and Distributed MTDC method separately, meanwhile 14 Bus MTDC-AC hybrid system and 30 bus hybrid MTDC-AC system are taken as test system. Simulation results have shown that the smoothness is optimal by using distributive approach, compared to solving the problem with the centralized OPF method and centralized hybrid-MTDC method.

REFERENCES

[1] H.-Z. Wang, G.-Q. Li, G.-B. Wang, J.-C. Peng, H. Jiang, and Y.-T. Liu, "Deep learning based ensemble approach for probabilistic wind power forecasting," *Appl. Energy*, vol. 188, pp. 56–70, Feb. 2017.

[2] H. Wang, H. Yi, J. Peng, G. Wang, Y. Liu, H. Jiang, and W. Liu, "Deterministic and probabilistic forecasting of photovoltaic power based on deep convolutional neural network," *Energy Convers. Manage.*, vol. 153, pp. 409–422, Dec. 2017.

[3] H. Wang, J. Ruan, G. Wang, B. Zhou, Y. Liu, X. Fu, and J. Peng, "Deep learning-based interval state estimation of AC smart grids against sparse cyber attacks," *IEEE Trans. Ind. Informat.*, vol. 14, no. 11, pp. 4766–4778, Nov. 2018.

[4] F. Dalir, M. S. Motlagh, and K. Ashrafi, "A dynamic quasi comprehensive model for determining the carbon footprint of fossil fuel electricity: A case study of Iran," *J. Cleaner Prod.*, vol. 188, pp. 362–370, Jul. 2018.

[5] K. Das, A. Nitsas, M. Altin, A. D. Hansen, and P. E. Sørensen, "Improved load-shedding scheme considering distributed generation," *IEEE Trans. Power Del.*, vol. 32, no. 1, pp. 515–524, Feb. 2017.

[6] H. Liao and J. V. Milanović, "Methodology for the analysis of voltage unbalance in networks with single-phase distributed generation," *IET Gener., Transmiss. Distrib.*, vol. 11, no. 2, pp. 550–559, Jan. 2017.

[7] B. R. Pereira, G. R. Martins da Costa, J. Contreras, and J. R. S. Mantovani, "Optimal distributed generation and reactive power allocation in electrical distribution systems," *IEEE Trans. Sustain. Energy*, vol. 7, no. 3, pp. 975–984, Jul. 2016.

[8] S. Mirsaeidi, X. Dong, and D. M. Said, "Towards hybrid AC/DC microgrids: Critical analysis and classification of protection strategies," *Renew. Sustain. Energy Rev.*, vol. 90, pp. 97–103, Jul. 2018.

[9] A. K. Singh and S. K. Parida, "A review on distributed generation allocation and planning in deregulated electricity market," *Renew. Sustain. Energy Rev.*, vol. 82, pp. 4132–4141, Feb. 2018.

[10] J. Liu, H. Cheng, P. Zeng, L. Yao, C. Shang, and Y. Tian, "Decentralized stochastic optimization based planning of integrated transmission and distribution networks with distributed generation penetration," *Appl. Energy*, vol. 220, pp. 800–813, Jun. 2018.

[11] N. M. Sapari, H. Mokhlis, J. A. Laghari, A. H. A. Bakar, and M. R. M. Dahalan, "Application of load shedding schemes for distribution network connected with distributed generation: A review," *Renew. Sustain. Energy Rev.*, vol. 32, pp. 858–867, Feb. 2018.

[12] H. Ji, C. Wang, P. Li, G. Song, and J. Wu, "SOP-based islanding partition method of active distribution networks considering the characteristics of DG, energy storage system and load," *Energy*, vol. 155, pp. 312–325, Jul. 2018.

[13] E. Shoubaki, S. Essakiappan, M. Manjrekar, and J. Enslin, "Synthetic inertia for BESS integrated on the DC-link of grid-tied PV inverters," in *Proc. IEEE 8th Int. Symp. Power Electron. Distrib. Gener. Syst. (PEDG)*, Apr. 2017, pp. 1–5.

[14] T. Adefarati and R. C. Bansal, "Integration of renewable distributed generators into the distribution system: A review," *IET Renew. Power Gener.*, vol. 10, no. 7, pp. 873–884, Jul. 2016.

[15] M. T. Alam and Q. Ahsan, "A mathematical model for the transient stability analysis of a simultaneous AC–DC power transmission system," *IEEE Trans. Power Syst.*, vol. 33, no. 4, pp. 3510–3520, Jul. 2018.

[16] S. Yu, S. Zhang, Y. Wei, Y. Zhu, and Y. Sun, "Efficient and accurate hybrid model of modular multilevel converters for large MTDC systems," *IET Gener. Transmiss. Distrib.*, vol. 12, no. 7, pp. 1565–1572, Apr. 2018.

[17] J. Renedo, A. García-Cerrada, and L. Rouco, "Active power control strategies for transient stability enhancement of AC/DC grids with VSC-HVDC multi-terminal systems," *IEEE Trans. Power Syst.*, vol. 31, no. 6, pp. 4595–4604, Nov. 2016.

[18] A. T. Elsayed, A. A. Mohamed, and O. A. Mohammed, "DC microgrids and distribution systems: An overview," *Electr. Power Syst. Res.*, vol. 119, pp. 407–417, Feb. 2015.

[19] W. Zhao, S. Li, L. Qin, and Y. Huang, "The stability study and simulation analysis on multi-infeed AC-DC hybrid power system," in *Proc. 5th IEEE Int. Conf. Electr. Utility Deregulation, Restructuring Power Technol. (DRPT)*, Nov. 2015, pp. 557–562.

[20] M. Szechtman, M. J. Ximenes, and A. R. Saavedra, "Comparative analysis of stability and electromagnetic transient studies for HVDC multi-infeed systems," *CSEE J. Power Energy Syst.*, vol. 3, no. 3, pp. 253–259, Sep. 2017.

[21] J. Yang, Z. He, J. Ke, and M. Xie, "A new hybrid multilevel DC–AC converter with reduced energy storage requirement and power losses for HVDC applications," *IEEE Trans. Power Electron.*, vol. 34, no. 3, pp. 2082–2096, Mar. 2019.

[22] S. Cao, W. Xiang, L. Yao, B. Yang, and J. Wen, "AC and DC fault ride through hybrid MMC integrating wind power," *J. Eng.*, vol. 2017, no. 13, pp. 828–833, 2017.

[23] Z. Hai-Lin, Y. Shu-Jun, and Z. Peng, "Research on small-signal stability of hybrid multi-terminal HVDC system and control system parameter design," *J. Eng.*, vol. 2017, no. 13, pp. 2401–2406, 2017.

[24] Y. Zhang, K. Gao, Z. Han, P. Yu, Y. Chen, and J. Ma, "Multi-objectives OPF of AC-DC systems considering VSC-HVDC integration," in *Proc. Asia–Pacific Power Energy Eng. Conf. (APPEEC)*, Oct. 2016, pp. 929–933.

[25] S. Gao, H. Ye, Y. Du, and H. Liu, "A general decoupled AC/DC power flow algorithm with VSC-MTDC," in *Proc. 13th IEEE Conf. Ind. Electron. Appl. (ICIEA)*, May/Jun. 2018, pp. 1779–1784.

[26] Y. Li, Z. Xu, J. Østergaard, and D. J. Hill, "Coordinated control strategies for offshore wind farm integration via VSC-HVDC for system frequency support," *IEEE Trans. Energy Convers.*, vol. 32, no. 3, pp. 843–856, Sep. 2017.

[27] C. Gavriluta, I. Candela, C. Citro, A. Luna, and P. Rodriguez, "Decentralized control of MTDC networks with energy storage and distributed generation," in *Proc. IEEE Energy Convers. Congr. Expo.*, Sep. 2013, pp. 2657–2663.

[28] M. Aragüés-Peñalba, A. Egea-Àlvarez, O. Gomis-Bellmunt, and A. Sumper, "Optimum voltage control for loss minimization in HVDC multi-terminal transmission systems for large offshore wind farms," *Electr. Power Syst. Res.*, vol. 89, pp. 54–63, Aug. 2012. [Online]. Available: http://www.sciencedirect.com/science/article/pii/S0378779612000478

[29] T. K. Vrana, J. Beerten, R. Belmans, and O. B. Fosso, "A classification of DC node voltage control methods for HVDC grids," *Electr. Power Syst. Res.*, vol. 103, pp. 137–144, Oct. 2013.

[30] A. R. Malekpour, A. Pahwa, and B. Natarajan, "Hierarchical architecture for integration of rooftop PV in smart distribution systems," *IEEE Trans. Smart Grid*, vol. 9, no. 3, pp. 2019–2029, May 2018.

[31] S. Aziz, H. Jiang, J.-C. Peng, J.-Q. Ruan, and H.-Z. Wang, "Optimization of base operation points of MTDC grid for improving transition smooth," in *Proc. IEEE Conf. Energy Internet Energy Syst. Integr.*, Nov. 2017, pp. 1–6.

[32] G. Andersson, "Modelling and analysis of electric power systems," EEH-Power Syst. Lab., Zurich, Switzerland, 2008.

[33] R. Baldick, B. H. Kim, C. Chase, and Y. Luo, "A fast distributed implementation of optimal power flow," *IEEE Trans. Power Syst.*, vol. 14, no. 3, pp. 858–864, Aug. 1999.
[34] E. Dall'Anese, H. Zhu, and G. B. Giannakis, "Distributed optimal power flow for smart microgrids," *IEEE Trans. Smart Grid*, vol. 4, no. 3, pp. 1464–1475, Sep. 2013.
[35] J. Nocedal and S. Wright, *Numerical Optimization*. New York, NY, USA: Springer, 2006.
[36] R. Zimmerman and D. Gan. (Dec. 2016). *MATPOWER: A MATLAB Power System Simulation Package*. [Online]. Available: http://www.pserc.cornell.edu

SADDAM AZIZ received the B.Eng. degree and M.Eng. degree in electrical engineering from Chongqing University, Chongqing, China, in 2012 and 2015, respectively. He is currently pursuing the Ph.D. degree with the Department of Mechatronics and Control Engineering, Shenzhen University, Shenzhen, China. His research interests mainly include multi-terminal DC system operation, optimization, and planning.

JIANCHUN PENG (M'04–SM'17) received the B.S. and M.S. degrees from Chongqing University, Chongqing, China, in 1986 and 1989, respectively, and the Ph.D. degree from Hunan University, Hunan, China, in 1998, all in electrical engineering. He was a Visiting Professor, from 2002 to 2003 with Arizona State University, Tempe, and from 2006 to 2006, with Brunel University, London, U.K. He is currently a Professor with Shenzhen University and the Director of the Department of Control Science and Engineering. His interests include electricity markets, power system optimal operation, and control.

HUAIZHI WANG (M'16) received the B.Eng. and M.Eng. degrees in control science and engineering from Shenzhen University, Shenzhen, China, in 2009 and 2012, respectively, and the Ph.D. degree in electrical engineering from the South China University of Technology, Guangzhou, China, in 2015. He was a Research Assistant with the Department of Electrical Engineering, Hong Kong Polytechnic University, Hong Kong, from 2014 to 2015. He is currently an Assistant Professor with Shenzhen University, Shenzhen, China. His research mainly focuses on automatic generation control in cyber physical power system.

HUI JIANG received the B.S. degree from Chongqing University, Chongqing, China, in 1990, and the M.S. and Ph.D. degrees from Hunan University, Hunan, China, in 1999 and 2005, respectively, all in electrical engineering. From 2005 to 2006, she was a Visiting Scholar at Brunel University, London, U.K. She is currently a Professor with Shenzhen University. Her interests include power system economics, and power system planning and operation.